

## **Effect of Shape, Size of Pores on Saturated Hydraulic Conductivity of Some Iraqi Soils**



**A. S. Ati<sup>\*</sup>, B. M. Kareem<sup>\*\*</sup>**

<sup>\*</sup>Dep. of Soil Science and Water Resources, University of Baghdad-  
College of Agriculture, Baghdad, Iraq, e-mail: salih\_alaa@yahoo.com

<sup>\*\*</sup>Dep. of Soil Science and Water Resources, University of Baghdad-College of  
Agriculture, Baghdad, Iraq

### **Abstract:**

This study aims to find out the effect of shape, size of pores on saturated hydraulic conductivity. Ten pedons were selected from the north of Iraq; five pedons were selected from Sulamani province: Bakhteari forest, Bazian, Choesoor, Kanakow and Sarsank was from Duhok province. While in the middle sites, five pedons were selected from Baghdad, two from college of agriculture, Al-Tarmia, and Al-Raeed experimental station, the last pedon from Al-Anbar province – Al-Husaenia. Disturbed and undisturbed soil samples were taken from surface and subsurface horizons from each pedon. Some chemical and physical properties were determined, which include texture, carbonate minerals, free iron oxides, organic matter, bulk density, porosity and hydraulic conductivity. Also they were used for micro morphological characterization as thin section and scanning electron microscopy. The results indicated that the highest value of saturated hydraulic conductivity of the northern sites were  $77.73 \text{ cm.hr}^{-1}$  at  $P_4A_1$  (north), the lowest value was  $0.47$  and  $0.47 \text{ cm.hr}^{-1}$  observed in surface and subsurface horizons of  $P_3$ . The high value of middle sites was  $9.89 \text{ cm.hr}^{-1}$  in  $P_9A_1$ ; the lowest value was  $0.89 \text{ cm.hr}^{-1}$  in  $P_8C_1$ . Micro morphological characterization showed variation in the shapes and size of pores for all studied horizons. Also, they showed coating and filling material affecting the pores. The dominant shapes were channels, chambers, voids. The results show that there are differences in shapes and size of pores between north and middle sites, where the dominant shapes of pores in middle sites were chamber and packing. The results showed the existence of free iron oxides which increased MWD and bulk density and decrease hydraulic conductivity and porosity; also it's forming type of shape as small chamber. Organic matter forms meta vughs which make the hydraulic conductivity high because this type of shape is more stable.

**Keywords:** hydraulic conductivity; shape and size of pores; micro morphological; scanning electron microscopy

### **I. Introduction:**

Hydraulic conductivity is one of the most important soil physical properties for determining infiltration rate, irrigation and drainage practices, and other hydrological processes [1,2]. Some soil physical characteristics that influence the

hydraulic conductivity are the total porosity, pore size distribution and geometry of the soil. Any factor effects arrangement, size distribution of soil pores, will have an effect on hydraulic conductivity [3]. Hydraulic conductivity is dependent on total porosity, pores-size

distribution, tortuosity and the ratio of the average length of the pore passage and total porosity [4, 5].

Soil thin section analysis and dye application in intact soils are the most common techniques for studying soil structure, porosity, and transport parameters [6, 7, 8]. The application of image analysis techniques to determine pore characteristics and soil structure in thin section has become an indispensable tool for research in soil science [9]. The characterization of the porous network from the image analysis of soil thin section allows an independent and direct evaluation of the water dynamic in a structured soil [10, 11]. This technique has been used to measure the pore size distribution in the various soil horizons [12] to characterize the orientation, shape, and size of different pores [13], and to quantify dye transport in preferential flow pathways [14, 15]. Shape and size of pores and void regulation are responsible for water movement among soil material, is vary important in soil format [16].

Pore system with micropores and their impact on saturated hydraulic conductivities were previously explored by [17] Soil porosity is usually examined on thin section, using various image analysis techniques [18]. The objective of this study was to investigate the effect of cementing materials (e.g. carbonate minerals, free iron oxides and organic matter) on saturated hydraulic conductivity as reflected with total soil pores and micro morphological characteristics.

## **II. Material and Methods:**

Soil samples were collected from ten different locations from Iraq. These samples were varying in their: (i) carbonate minerals, (ii) iron oxides, and

(iii) organic matter. Ten soil pedons were excavated from these ten locations:

- |             |  |
|-------------|--|
| Pedon No.1  | Kanakaw – Suleimaniya province               |
| Pedon No.2  | Bakhtyari forest – Suleimaniya province      |
| Pedon No.3  | Chowsoor – Suleimaniya province              |
| Pedon No.4  | Bazian – Suleimaniya province                |
| Pedon No.5  | Sarsang – Duhok province                     |
| Pedon No.6  | College of Agriculture – Baghdad province    |
| Pedon No.7  | College of Agriculture – Baghdad province    |
| Pedon No.8  | Al- Raid Experimental station – Baghdad pro. |
| Pedon No.9  | Al- Tarmai –Baghdad province                 |
| Pedon No.10 | Al- Husainia / Al – Anbar province           |

All pedons were morphologically described according to [19]. Twenty surfaces and subsurface soil samples were taken including disturbed and undisturbed soil samples from each horizon. Disturbed soil samples were air- dried and passed through a sieve of 2000  $\mu\text{m}$  to determine chemical, physical, micromorphological and clay minerals and 4000- 9000  $\mu\text{m}$  sieve to determine aggregate stability parameters. Some chemical and physical characteristics are presented in Tables 1 and 2. Laboratory determination of  $K_{sat}$  was done using the constant head method as described by [20]. Thin section for soil materials, has been done according to [16] method, (all the work had been accomplished in the Faculty of Science- Baghdad University- Department of Earth Sciences). Preparation of clay sample for X-ray analysis according to [21]. Organic matter was determined by method of [22]. Calcium carbonate minerals ( $\text{CaCO}_3$ ) were determined by hydrochloric acid (3N), using the calcimeter procedure [23] Total free oxides were extracted using the CBD

(citrate- bicarbonate - Na-dithionite), according to [24]. The same thin sections slides were examined by Scanning Electron Microscopy (SEM) at the

laboratories of Earth and Environment School, University of Western Australia. Statistical analysis was estimated by [25]

Table.I: Some soil chemical characteristics of the studied pedons.

Pedon	Horizon	EC (dS.m <sup>-1</sup> )	pH	Cmol. l <sup>-1</sup>				Ca <sup>+2</sup> /Mg <sup>+2</sup>
				Ca <sup>+2</sup>	Mg <sup>+2</sup>	Na <sup>+</sup>	K <sup>+</sup>	
P <sub>1</sub>	A <sub>1</sub>	0.55	8.40	0.62	1.25	0.02	0.01	0.50
	B	0.54	8.25	0.51	0.11	0.08	0.01	4.60
P <sub>2</sub>	A <sub>1</sub>	0.40	7.89	0.70	0.20	0.02	0.01	3.50
	B	0.32	7.61	0.70	0.22	0.19	0.01	3.20
P <sub>3</sub>	A <sub>1</sub>	0.25	8.33	0.87	0.30	0.05	0.21	2.90
	B <sub>t</sub>	0.57	8.02	0.51	0.11	0.08	0.04	4.60
P <sub>4</sub>	A <sub>1</sub>	0.27	8.24	0.57	0.05	0.03	0.16	11.40
	B <sub>k</sub>	0.82	8.03	0.82	0.60	0.30	0.01	1.40
P <sub>5</sub>	A	0.44	8.00	0.71	0.23	0.02	0.05	3.10
	B <sub>k</sub>	0.30	8.43	0.51	0.35	0.03	0.01	1.40
P <sub>6</sub>	A <sub>1</sub>	1.30	8.40	5.10	2.70	1.20	0.80	1.90
	C <sub>1</sub>	3.70	8.05	1.60	1.10	0.50	0.30	1.40
P <sub>7</sub>	A <sub>1</sub>	19.30	7.39	53.00	45.80	95.10	0.10	1.16
	C <sub>1</sub>	7.00	7.35	22.10	29.30	18.40	0.30	0.75
P <sub>8</sub>	A <sub>1</sub>	28.13	7.71	69.50	60.10	150.10	1.00	1.16
	C <sub>1</sub>	5.90	7.80	24.30	16.50	17.20	0.50	1.47
P <sub>9</sub>	A <sub>1</sub>	0.91	8.41	4.00	2.60	1.80	0.01	1.54
	C <sub>1</sub>	0.52	8.37	2.00	2.50	0.90	0.01	0.80
P <sub>10</sub>	A <sub>1</sub>	0.60	8.16	0.72	0.43	0.311	0.01	1.67
	C <sub>1</sub>	0.70	8.33	0.67	0.36	0.23	0.01	1.86

Table.II: Particle size distribution for the studied pedons.

Pedon	Horizon	Particle size distribution (with CaCO <sub>3</sub> ) g. kg <sup>-1</sup>				Texture Class	Particle size distribution (without CaCO <sub>3</sub> ) g.kg <sup>-1</sup>			
		Clay	Silt	Sand	Texture Class		Clay	Silt	Sand	Texture Class
P <sub>1</sub>	A <sub>1</sub>	556.2	390.4	53.4	C	562.3	386.5	51.3	C	
	B	594.9	359.4	45.6	C	620.0	343.5	36.6	C	
P <sub>2</sub>	A <sub>1</sub>	474.3	418.8	106.7	Si L	551.8	397.7	50.5	C	
	B	377.8	494.8	127.5	Si C L	571.9	381.4	46.6	C	
P <sub>3</sub>	A <sub>1</sub>	135.5	232.5	632.1	S L	212.1	254.1	533.9	SCL	
	B <sub>t</sub>	140.1	600.7	259.3	Si L	253.1	594.5	152.4	Si L	
P <sub>4</sub>	A <sub>1</sub>	567.6	386.3	47.8	C	607.7	357.4	34.9	C	
	B <sub>k</sub>	520.8	388.7	90.3	C	619.1	358.3	22.6	C	
P <sub>5</sub>	A	403.4	311.2	285.4	C L	534.2	183.8	282.0	C	
	B <sub>k</sub>	95.8	254.4	649.8	S L	377.1	135.2	487.8	SC	
P <sub>6</sub>	A <sub>1</sub>	312.4	507.2	180.4	Si C L	373.2	456.1	170.8	Si C L	
	C <sub>1</sub>	363.2	443.2	193.7	Si C L	323.8	498.3	178.0	Si C L	
P <sub>7</sub>	A <sub>1</sub>	389.3	416.5	194.2	Si C L	384.7	422.8	192.6	Si C L	
	C <sub>1</sub>	323.8	504.7	171.5	Si L	391.1	439.7	169.2	Si C L	
P <sub>8</sub>	A <sub>1</sub>	220.7	609.3	170.1	Si L	295.2	544.5	160.4	Si C L	
	C <sub>1</sub>	219.4	570.3	210.4	Si L	269.7	521.8	208.5	Si L	
P <sub>9</sub>	A <sub>1</sub>	259.5	377.3	363.2	C L	274.3	436.6	289.1	C L	
	C <sub>1</sub>	170.6	559.3	270.5	Si L	284.2	489.7	226.2	C L	
P <sub>10</sub>	A <sub>1</sub>	131.0	289.3	579.5	S L	135.9	285.4	578.6	S L	
	C <sub>1</sub>	152.4	346.3	503.5	L	154.5	341.8	501.5	L	

### III. Result and Discussion:

Table 3 shows the hydraulic conductivity values for all studied sites. It well know that hydraulic conductivity depends strongly on texture and pore size distribution, however in some sites had similar texture but differ in  $K_{ast}$ . This may be attributed to other factors such as cementing agents and their interaction. Consequently, they also affect shape, size and distribution of pores. The highest values of  $K_{ast}$  in studied sites were 77.73 and 3.77  $\text{cm.hr}^{-1}$  recorded in surface and subsurface horizons of  $P_4$  pedon, respectively. While the lowest value was 0.47  $\text{cm. hr}^{-1}$  observed in surface and subsurface horizons of  $P_3$ . The reason of upturn value in  $P_4A_1$  was the effect of organic matter content which led to decrease the bulk density and lower porosity, MWD and GMD (Tables 3&4), and cause to many differences in shapes of pores (Fig. 4 Plate  $P_4A_1$ ). While, the decrease of  $K_{ast}$  in  $P_3$  was due to free iron oxides content, casing to developed soil structure, and increasing of MWD and GMD, at the meantime bulk density was increased with decreasing in porosity of the surface horizon. It also, increases the bulk density in subsurface horizon, with a decrease in MWD and a decrease in porosity as compared with the surface horizons. The decrease in  $K_{ast}$  might be attributed to the role of free iron oxides which in turn reduces and closes pores, that contributes to consolidation [26] Also, [27] showed that deposition of iron oxides in narrow necks of conducting pores reduced the soil's hydraulic conductivity. The low  $K_{sat}$  values in  $P_3$  attributed to low  $\text{Ca}^{2+}/\text{Mg}^{2+}$  ratio. The low  $\text{Ca}^{2+}/\text{Mg}^{2+}$  ratio and high contents caused dispersion in  $P_3$ . Saturated hydraulic conductivities of  $P_3$  were lower than these of  $P_4$ . Of is most

probably due to low  $\text{Ca}^{2+}/\text{Mg}^{2+}$  ratio in  $P_3$ . This was well matched to results of [28] who found that low  $\text{Ca}^{2+}/\text{Mg}^{2+}$  ratios and high  $\text{Mg}^{2+}$  contents causing dispersion in soils. Results in Tables 1 and 3 showed that subsurface horizon in  $P_4$  had low  $\text{Ca}^{2+}/\text{Mg}^{2+}$  ratio (1.36) than surface horizon (11.4), whereas saturated hydraulic conductivity of the surface horizon (77.73  $\text{cm.hr}^{-1}$ ) was 60 to 70 times higher than these of the subsurface horizon (3.77  $\text{cm.hr}^{-1}$ ). Some differences been in  $K_{sat}$  between surface and subsurface horizons in  $P_1$ , the values were 9.89 and 2.07  $\text{cm.hr}^{-1}$ , respectively, reflected the effective of MWD which was higher in surface comparing with subsurface horizon, in addition to the role of root system of vegetation. Result showed that value of  $K_{sat}$  in surface horizon of  $P_2$  was low and increased with depth, recorded 1.41 and 5.65  $\text{cm.hr}^{-1}$ , respectively. The increase in  $K_{sat}$  of subsurface horizon was due to calcium carbonates content which led to increase in MWD, GMD. Organic matter content has been higher in surface horizon in than the subsurface horizon and having close values of bulk density, MWD, and porosity. The interaction between clay minerals and organic matter led to swelling of clays, which in turn led to decrease in  $K_{sat}$ ; therefore clay minerals have been analyzed by XRD analysis. Fig.11 showed the dominant clay mineral was smectite as detected from peaks at (14.79, and 16.69  $\text{A}^\circ$ ) in Mg-saturated-air dry and ethylene glycol treatments, respectively. While, the (14.79  $\text{A}^\circ$ ) peak was disappeared when saturated samples with  $\text{K}^+$ -and heated to (550 $^\circ\text{C}$ ). These results approved that smectite was a dominant mineral in clay fraction of studied soils. The swelling ability of smectite in these soils caused to reduce size of pores and changing their

shapes, which in turn decreased the  $K_{sat}$ . Hence, channel type of pores was common in surfaces horizons, exposing them to more precipitation of calcium carbonates

and clay particles which closes them and decreases water movement (Fig.2 plat P<sub>2</sub>A<sub>1</sub>).

Table.III: Mean Weight Diameter (MWD), Geometric Mean Diameter (GMD), Bulk Density ( $\rho_b$ ), Total Porosity ( $f$ ) and Hydraulic Conductivity ( $K_{sat}$ ) of studied pedon.

Pedon	Horizon	MWD (mm)	GMD (mm)	$\rho_b$ (Mg.m <sup>-3</sup> )	$f$ (%)	$K_{sat}$ (cm.hr <sup>-1</sup> )
P <sub>1</sub>	A <sub>1</sub>	2.24	0.92	1.44	44.54	9.89
	B	0.50	0.61	1.35	47.95	2.07
P <sub>2</sub>	A <sub>1</sub>	1.62	0.91	1.37	47.39	1.41
	B	1.84	1.15	1.39	46.68	5.65
P <sub>3</sub>	A <sub>1</sub>	3.52	1.22	1.49	43.63	0.47
	B <sub>t</sub>	1.40	0.84	1.41	46.7	0.47
P <sub>4</sub>	A <sub>1</sub>	2.45	1.13	1.19	54.07	77.73
	B <sub>k</sub>	1.18	0.84	1.55	40.44	3.77
P <sub>5</sub>	A	1.63	0.88	1.26	51.67	12.72
	B <sub>k</sub>	6.10	2.03	1.32	49.17	32.98
P <sub>6</sub>	A <sub>1</sub>	1.35	0.82	1.29	50.56	5.18
	C <sub>1</sub>	2.14	0.92	1.49	42.71	5.65
P <sub>7</sub>	A <sub>1</sub>	0.34	0.52	1.34	48.37	2.12
	C <sub>1</sub>	0.29	0.51	1.44	44.79	1.65
P <sub>8</sub>	A <sub>1</sub>	0.23	0.47	1.51	42.1	2.07
	C <sub>1</sub>	0.19	0.45	1.54	41.63	0.98
P <sub>9</sub>	A <sub>1</sub>	2.92	1.14	1.19	54.79	9.89
	C <sub>1</sub>	2.05	0.84	1.27	51.14	1.27
P <sub>10</sub>	A <sub>1</sub>	1.7	0.78	1.46	44.75	3.95
	C <sub>1</sub>	1.51	0.88	1.51	42.86	2.51
North Sites (mean)		2.25	1.05	1.38	47.22	14.72
Middle Sites(mean)		1.27	0.73	1.40	46.37	3.53
LSD		0.49	0.12	0.04	1.61	6.55

Table.IV: Calcium carbonate (CaCO<sub>3</sub>), Iron oxides (Fe<sub>2</sub>O<sub>3</sub>) and Organic matter (OM) content of studied pedon.

Pedon	Horizon	CaCO <sub>3</sub>	Fe <sub>2</sub> O <sub>3</sub> g.kg <sup>-1</sup>	O.M
P <sub>1</sub>	A <sub>1</sub>	56.0	6.90	9.0
	B	103.4	8.72	7.6
P <sub>2</sub>	A <sub>1</sub>	163.2	2.15	19.4
	B	215.6	1.05	5.5
P <sub>3</sub>	A <sub>1</sub>	163.0	13.37	4.1
	B <sub>t</sub>	192.0	13.62	3.4
P <sub>4</sub>	A <sub>1</sub>	64.3	5.43	27.6
	B <sub>k</sub>	162.0	8.49	8.6
P <sub>5</sub>	A	193.0	6.56	11.4
	B <sub>k</sub>	394.0	3.36	7.6
P <sub>6</sub>	A <sub>1</sub>	231.0	1.12	15.2
	C <sub>1</sub>	247.0	1.52	7.6
P <sub>7</sub>	A <sub>1</sub>	220.0	1.22	4.8
	C <sub>1</sub>	246.0	1.05	3.8
P <sub>8</sub>	A <sub>1</sub>	196.0	1.31	3.8
	C <sub>1</sub>	218.0	1.46	2.1
P <sub>9</sub>	A <sub>1</sub>	185.0	0.87	17.3
	C <sub>1</sub>	202.0	1.22	7.9
P <sub>10</sub>	A <sub>1</sub>	181.0	1.94	2.1
	C <sub>1</sub>	215.0	2.51	1.9
North Sites(mean)		170.65	6.97	10.42
Middle Sites(mean)		214.10	1.42	6.65
LSD		26.42	1.16	2.51

From data mentioned above, we notice that  $K_{sat}$  value was higher in subsurface than surface horizon in P<sub>5</sub>, the recorded values were 32.98 and 12.72 cm.hr<sup>-1</sup>, respectively. In this case we might attributed the effect of calcium carbonates on soil separates by making aggregates strong which improves and increases of MWD, GMD and strengthen pores structure with different shapes of them as compared with surface horizon. The surface and subsurface horizons of P<sub>6</sub> were similar in  $K_{sat}$  values, where the values ranged from 5.18 to 5.65cm.hr<sup>-1</sup>,

respectively. The difference in values of  $K_{sat}$  was due to effect of calcium carbonates on MWD, and GMD especially in subsurface horizon, the mater that led to pores from the kind chamber with many differences sizes (Fig.6 plate, P<sub>6</sub>C<sub>1</sub>). Results showed that related to  $K_{sat}$  for P<sub>7</sub> and P<sub>8</sub>, was higher in surface horizons than subsurface horizons and values were 2.12, 1.65 and 2.07, 0.98 cm.hr<sup>-1</sup>, respectively. These sites are having close around values of bulk density, porosity, MWD, and GMD that reflects on  $K_{sat}$ .

Results showed that values of  $K_{sat}$  in  $P_9$  were higher in surface horizon than subsurface horizon, values were 9.89 and 1.27  $\text{cm.hr}^{-1}$ , respectively that was due to organic matter content, in addition to the tillage management, that led to decreasing the bulk density and increasing the porosity, MWD, and GMD as compared with subsurface horizon that aid to moderate of pores distribution and formed type of the chamber shapes pores (Fig 9 plate,  $P_9A_1$ ), consequently reflects on  $K_{sat}$ . While values of  $K_{sat}$  for  $P_{10}$  were 3.95 and 2.51  $\text{cm.hr}^{-1}$  observed in surface and subsurface horizon, respectively that was due to the increase in MWD, GMD and bulk density and the porosity and increase due to the effect of calcium carbonates on them and the porosity was decreased by precipitation of calcium carbonates and silt led to close and consolidation. In general the result in Table 3 displays that the values of  $K_{sat}$  for north sites were higher than middle sites, also we can noticed from data, the content of north sites of organic matter and free iron oxides were the highest and lowest in calcium carbonates content as compared with middle sites, hence the pedogenic processes of soil are higher, the matter that aid to form a great porosity and MWD which in turn caused many differences in kind of pores shapes, where they affect on  $K_{sat}$ .

The results of micromorphological studies for surface and subsurface horizons of all studied pedons can be considered as a complementary and support for chemical and physical properties. The morphological descriptions of thin section show the variation in the shapes and sizes of pores, that variation between surface and subsurface horizons. The podogenic processes are responsible for these variation, especially for the loose and addition of some soil materials. [29] found

that the size and shape of pores having impact on soil hydraulic are affected by coating and filling. Plates of  $P_1$  (Fig.1) and Fig.12 image of SEM exhibit that shape, size, and distribution of pores are different between surface and subsurface horizons, where the dominant shapes in surface horizons were interconnected chamber-channel and channels (Fig.1 Plate  $P_1A_1$ ), Shapes of channels are tubular smooth voids with a cylindrical or arched cross section which are uniform over much of the length. They are mainly root channels or biogalleries. These pores shapes were strongly and stable and can be attributed to the aggregate stability that affected by coating of clay and organic matter, hence roots system of plants which supported the shapes and size of pores that formed and reflects on  $K_{sat}$ . While, subsurface horizons (Fig.1 plate  $P_1B_1$ ), illustrated the existed chambers and meta vugh pores shapes where these shapes are more or equidimensional smooth-walled pores interconnected by channels, that depending on aggregates stability and cementing agents. Hence, this plate shows that the aggregates stability was the lowest, these pores are exposed to the blockage and precipitation which effected by coating and filling as well as clay and carbonates minerals do, especially in subsurface horizons. In case of  $P_2$  (Fig.2) and image of SEM plates of surface horizon refer to the existence of channels and planes shapes. Shapes of planes are flat voids, accommodation or not, smooth or rough, where they are the result of shrinkage slipping. Residual mold of plants roots and nodules of carbonates minerals are also existed. This horizon has lowest  $K_{sat}$  as in (Table 3) due to existed minerals of smectite groups which in turn cause swelling of soil that reduces the size and distribution of pores and it also changes

shapes, consequently the water movement through pathways are reduced, they were blocked and closed due to clay and carbonates minerals particles with coating and fillings of amorphous forms of calcium carbonates and calcite needles. The subsurface horizon was different from surface horizon, where plate of P<sub>2</sub>B<sub>1</sub> showed that the dominant shapes of pores is chambers that formed and existed due to role and act to the structure, that reflecting the role of cementing agent as well as carbonates minerals and clays, which is affect the pores structures and orientation of path ways that resulted in an increase of  $K_{sat}$  at this horizon as compared with surface horizon. Plates of P<sub>3</sub> for surface and subsurface horizons (Fig. 3) and Fig.14 images of SEM, where the dominant shapes were chambers and vesicles with moderately size distribution of pores in surface horizon (Fig.3 plate P<sub>3</sub>A<sub>1</sub>), where the existence of iron oxides reflects the structure that was shown in the values of MWD and GMD to be higher, the matter that causes a reduced size and disconnected pores. The tubular pores decreased values of  $K_{sat}$ . Subsurface horizon of P<sub>3</sub> (Fig. 3 plate P<sub>3</sub>B<sub>1</sub>) illustrates bigger size of pores with lower distribution where the dominant shapes were chambers, besides, the high content of iron oxides that has a role in enhancing structure that reflected on the shapes, and size of pores through out closing and blocking them, in addition to that, silt particles caused consolidation which affected the  $K_{sat}$  value [30].

The P<sub>4</sub> has the highest content of organic matter in surface horizon as compared with all horizons, where plate P<sub>4</sub>A<sub>1</sub> (Fig. 4) and Fig.15 images of SEM showed a meta vugh pores and shapes of channels, chambers, and compound packing types, that could be attributed to

the organic matter, which contributed creating connected and stable pathways, hence reflected on aggregate and porosity that gave the highest value of  $K_{sat}$  as compared with all other horizons. The Plate of subsurface horizon (P<sub>4</sub>B<sub>1</sub>) shows that pores size were smaller and lower than pores in plate P<sub>4</sub>A<sub>1</sub>, and they were shaped in a chamber like pores shape, although the iron oxides were nearly high which in turn increased aggregation (Tables 3 and 4). Also it was reflected on pathways to form a none uniform, disconnected, and narrow ones, therefore they were facing blockage by clay particles and iron oxides through out water movement that the HC was decreased as compared with surface horizon.

In plates of P<sub>5</sub> (Fig. 5) and Fig.16 image of SEM the surface horizon has been shown by plate P<sub>5</sub>A<sub>1</sub>, where the dominant shapes were chambers with low size distribution, besides the existence of carbonate minerals that resulted in forming these shapes and size that they might be attributed to the cementing agents especially carbonate minerals and clays which enhance the soil structure, and reflected on structure of pores, then after affecting the  $K_{sat}$ . The subsurface horizon of the same pedon has higher value of  $K_{sat}$  than surface horizon, in regard to the MWD and GMD where they were the highest from other horizons, plate P<sub>5</sub>B<sub>K</sub> shows existence of carbonates minerals that reflected on structure, that formed channels and small chambers pore shapes, in addition to that, carbonate minerals plays an important role to strengthen structure of pores and being more stable, uniform connected, with strong walls for that no precipitation of clay and other particles to close pathways among water movement occurred [29].

In regard to pales of  $P_6$ , the surface horizon has been a close of pores size distribution with subsurface horizon (Fig. 6), where the shapes in plate  $P_6A_p$  were complex packing voids and chambers, and that could be attributed to the role of organic matter, hence plant roots help structure in keeping these types of voids stable, while the plate of  $P_6C_1$  has been a mixed shapes of voids, that reflected the role of structure which reflected the cementing agents, where the MWD was higher than surface horizon, for that the pores are not affected highly by any coatings and fillings. The  $K_{sat}$  for both horizons were almost similar due to pores system and shapes. Plates of  $P_7$  and  $P_8$  exhibits close around or proximately matched of shapes and size distribution of pores (Fig. 7 and 8), where the dominant shapes were chambers and irregulars chambers, also the values of bulk density, MWD and GMD were also close, the matter that reflected on aggregates stability, therefore is blocking among precipitation soil material as well as clay or carbonate minerals that resulting in closing the pathways which reflected on  $K_{sat}$ . Plate of  $P_9$  (Fig. 9), the surface horizon has been a close of pores

distribution with subsurface horizons, where the shapes in plate  $P_9A_p$  were chambers, could be attributed to the role of organic matter, which help the structure to keep these types of voids of continuous and stable, this increased  $K_{sat}$  as compared with subsurface horizon, where the plate  $P_9C_1$  shows the dominant shapes were chambers, channels and inter connected channel-chamber, the low content of organic matter reflected on structure, therefore pores will be closed and disconnected due to precipitation soil material as silt and carbonate minerals that result to close the pathways and in turn decrease  $K_{sat}$ . In plate  $P_{10}$  (Fig. 10) shows the dominate shapes which were chambers, where plate ( $P_{10}A_1$ ) shows the existence precipitation of carbonate minerals and coating on particles, the matter that exposed the pores to the blockage and precipitation which effected by coating and filling. In the meantime for subsurface horizon (plate  $P_{10}C_1$ ), where the precipitation of carbonate minerals on the inner walls of pores besides, the increase of MWD and GMD were due to the existence of carbonate minerals that will make pathways are disconnected, and reflects on  $K_{sat}$ .

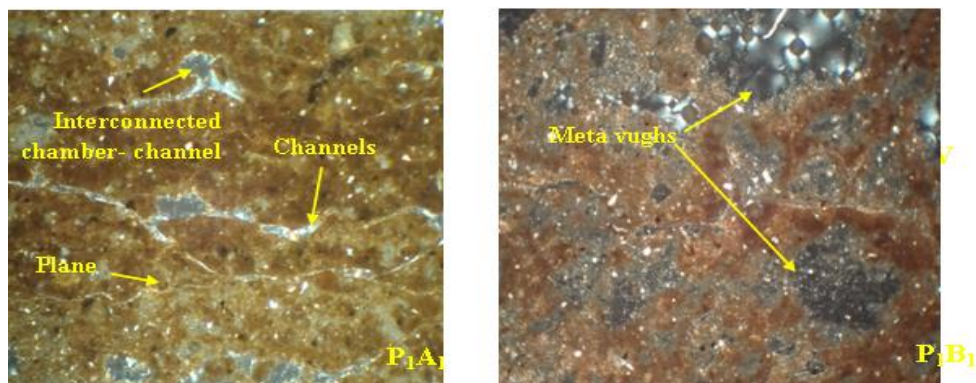


Fig. 1: Plate ( $P_1A_1$ ) ( $P_1B_1$ ) shows the dominant shapes (channel, plane, and inter connected chamber-channel), exists clay and (k) carbonate minerals. Plate ( $P_1B_1$ ) shows the dominant shapes (meta vughs).

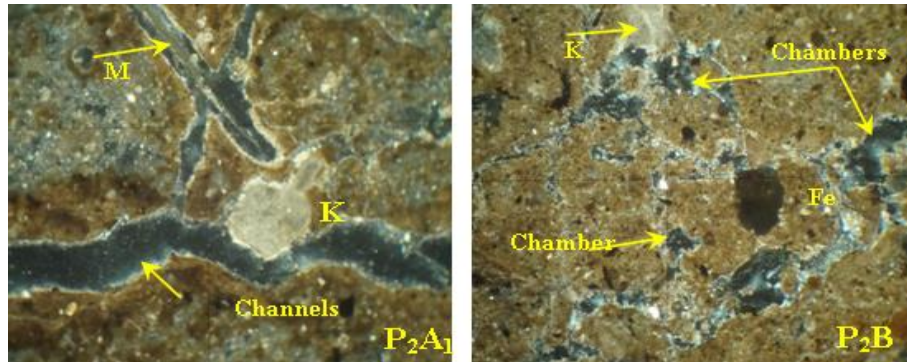


Fig. 2: Plate (P<sub>2</sub>A<sub>1</sub>) shows the dominant shapes (channel), exists (m) mold of plants roots and (k) carbonate minerals. Plate (P<sub>2</sub>B<sub>1</sub>) shows the dominant shapes (chambers), exists (Fe) iron oxides and (k) carbonate minerals.

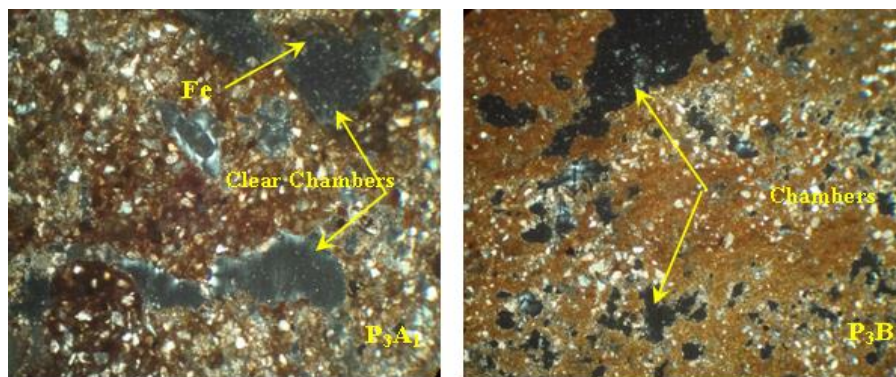


Fig. 3: Plate (P<sub>3</sub>A<sub>1</sub>) shows the dominant shapes (clear chambers), exists (Fe) iron oxides on walls of pores. Plate (P<sub>3</sub>B<sub>1</sub>) shows the dominant shapes (chambers), exists (Fe) iron oxides on walls of pores.

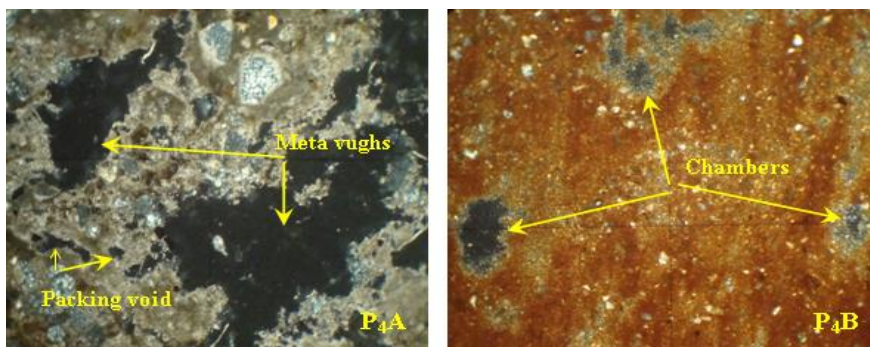


Fig. 4: Plate (P<sub>4</sub>A<sub>1</sub>) shows the dominant shapes (Meta vugh, chambers and compound packing). Plate (P<sub>4</sub>B<sub>1</sub>) shows the dominant shapes (small chambers).

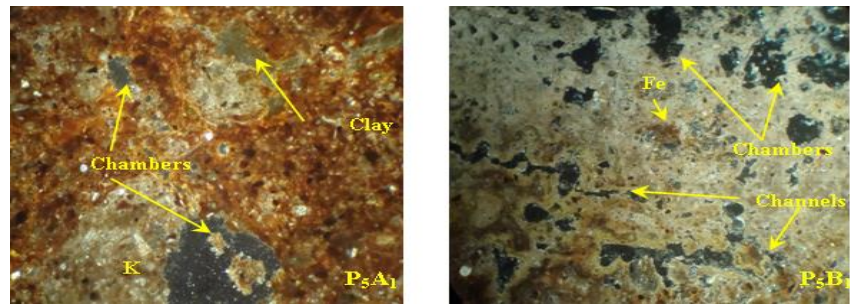


Fig. 5: Plate (P<sub>5A1</sub>) shows the dominant shapes (chamber), exists clay and (k) carbonate minerals. Plate (P<sub>5Bk</sub>) shows the dominant shapes (chamber and channel), exists (Fe) iron oxide.

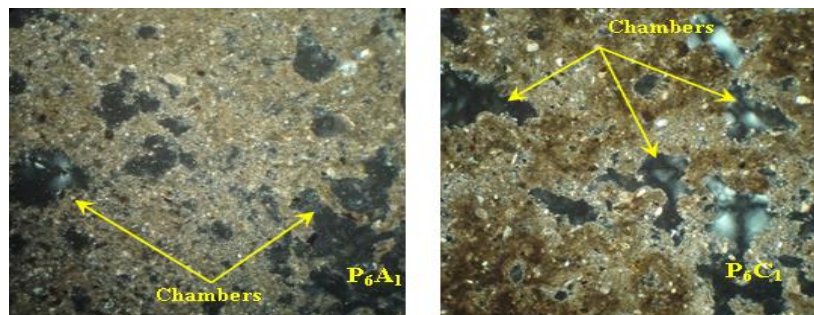


Fig. 6: Plate (P<sub>6A1</sub>) shows the dominant shapes (chambers). Plate (P<sub>6C1</sub>) shows the dominant shapes (chambers).

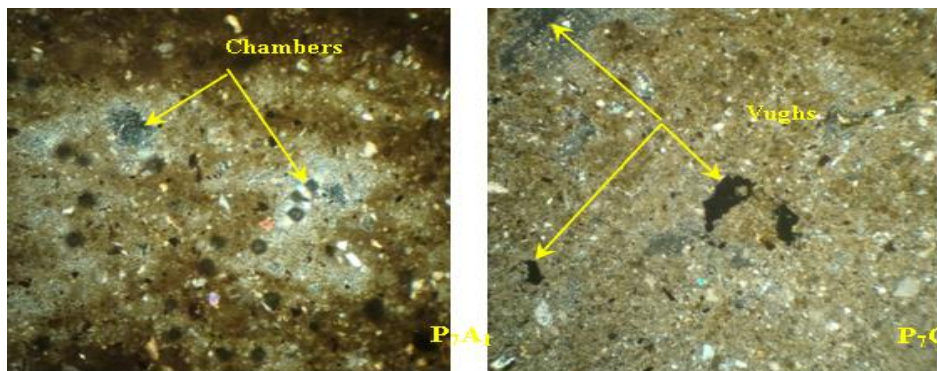


Fig. 7: Plate (P<sub>7A1</sub>) shows the dominant shapes (chambers). Plate (P<sub>7C1</sub>) shows the dominant shapes (vughs).

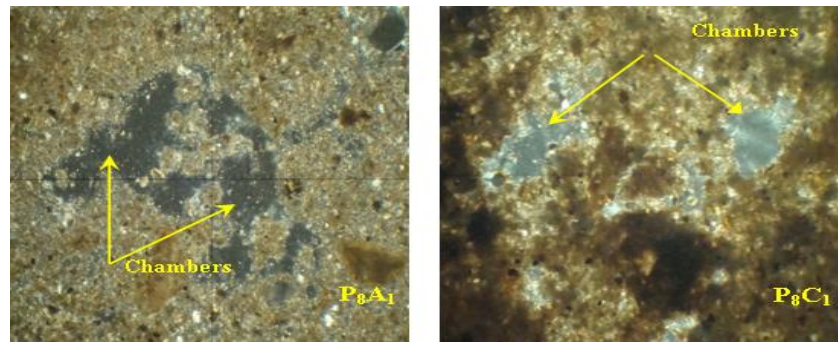


Fig. 8: Plate (P<sub>8</sub>A<sub>1</sub>) shows the dominant shapes (chambers). Plate (P<sub>8</sub>C<sub>1</sub>) shows the dominant shapes (chambers).

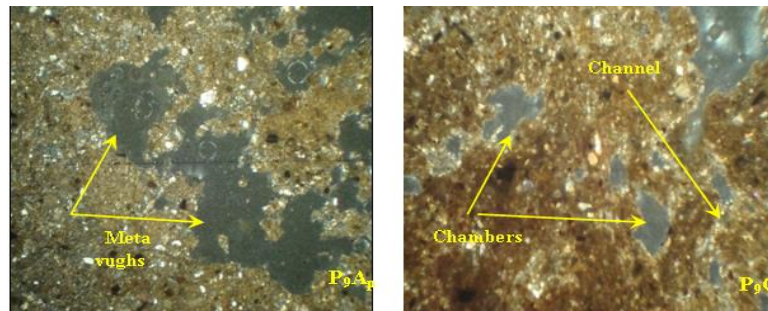


Fig. 9: Plate (P<sub>9</sub>A<sub>p</sub>) shows the dominant shapes (chambers). Plate (P<sub>9</sub>C<sub>1</sub>) shows the dominant shapes (channel, chambers).

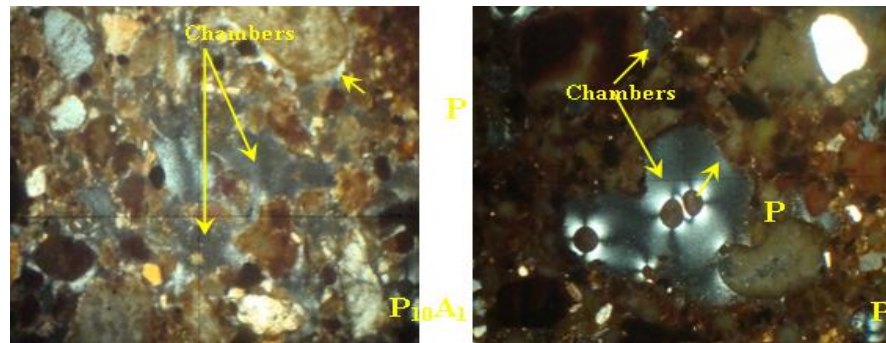


Fig. 10: Plate (P<sub>10</sub>A<sub>1</sub>) shows the dominant shapes (chambers), exists (P) precipitation of carbonate minerals and coating on particles. Plate (P<sub>10</sub>C<sub>1</sub>) shows the dominant shapes (chambers), exists (Q) quartz and (P) precipitation of carbonate minerals and coating on walls of pores.

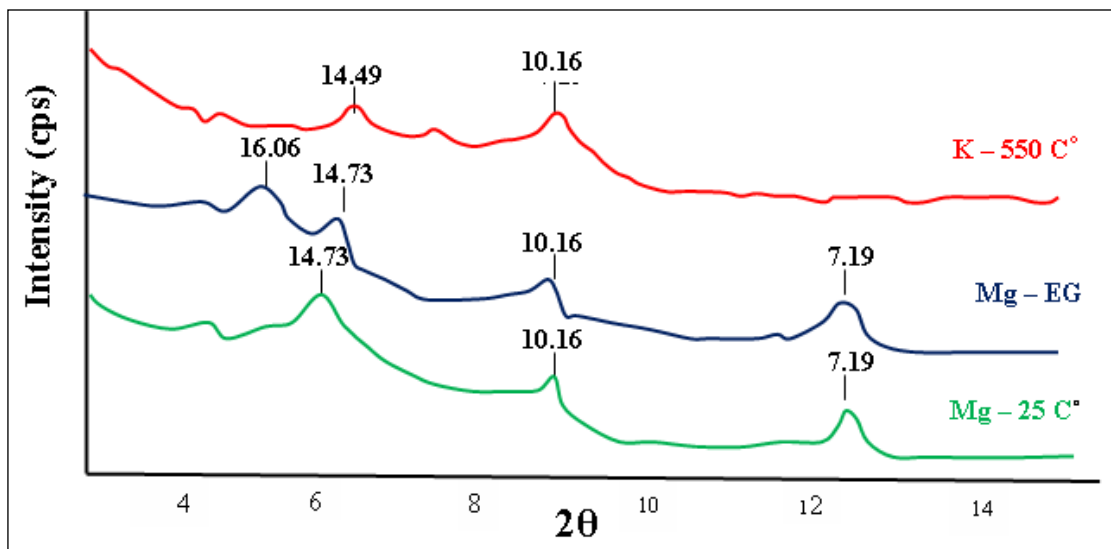


Fig. 11: The X – ray diffraction of clay separation for surface horizon of P<sub>2</sub>.

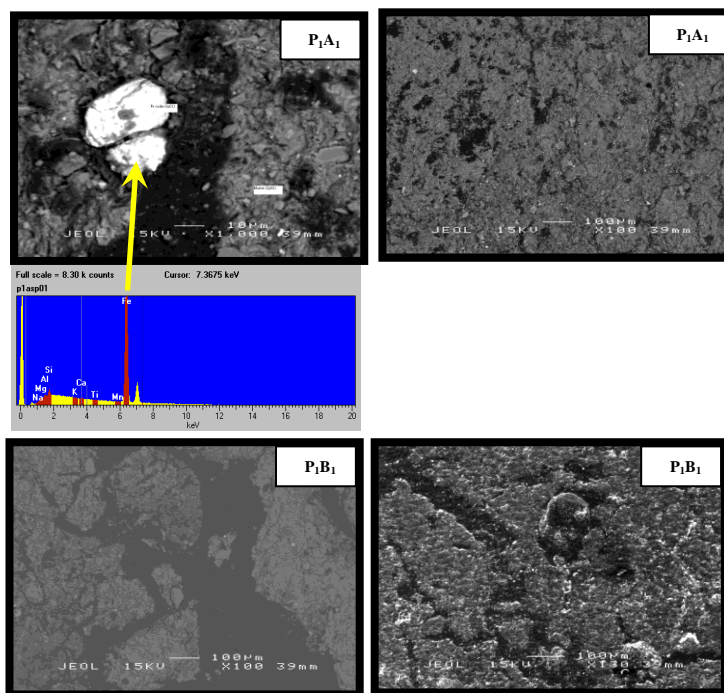


Fig. 12: Image of scanning electron microscopy (SEM) for surface and subsurface horizons of P<sub>1</sub>.

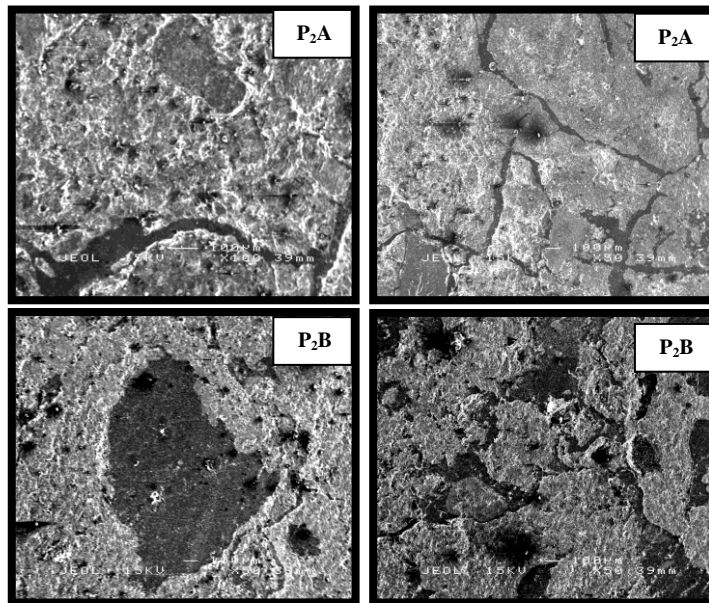


Fig. 13: Image of scanning electron microscopy (SEM) for surface and subsurface horizons of P<sub>2</sub>

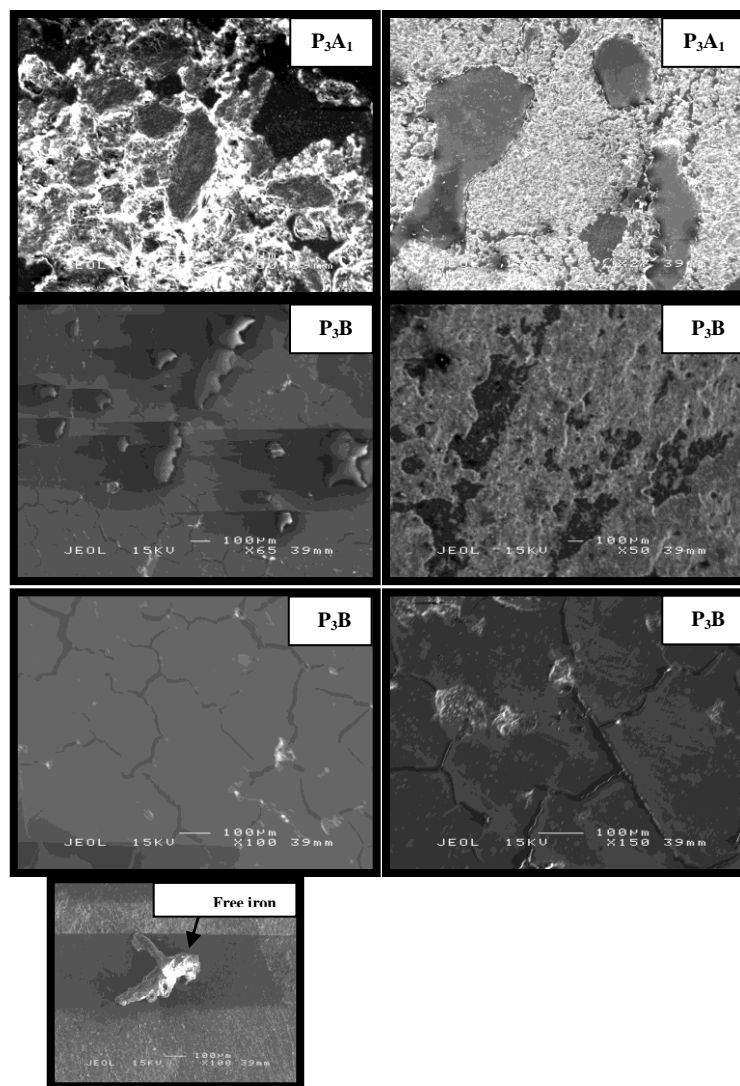


Fig. 14 Image of scanning electron microscopy (SEM) for surface and subsurface horizons of P<sub>3</sub>.

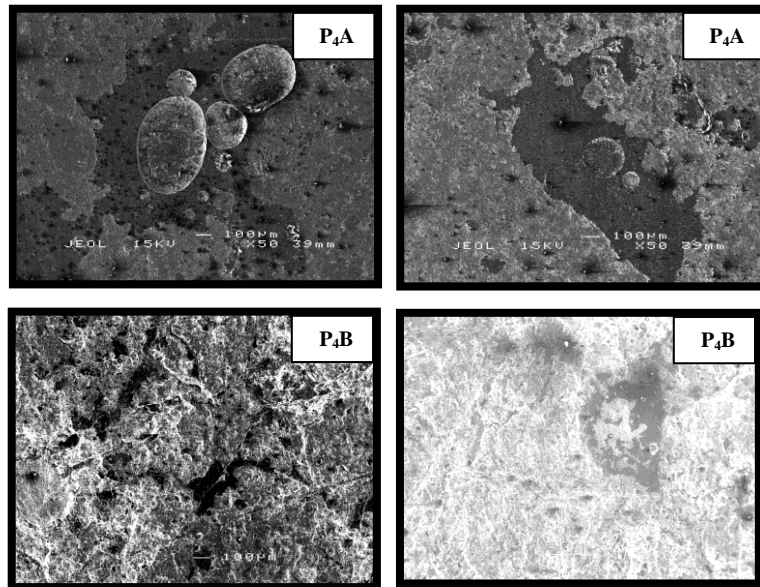


Fig. 15: Image of scanning electron microscopy (SEM) for surface and subsurface horizons of P<sub>4</sub>.

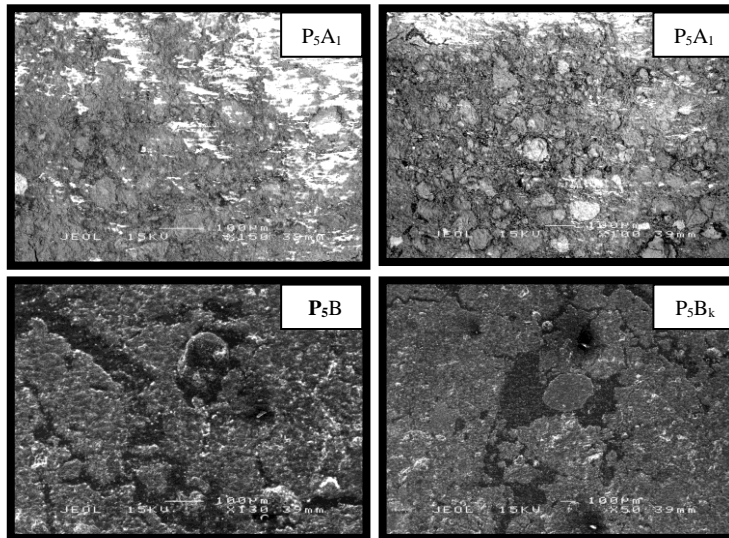


Fig. 16: Image of scanning electron microscopy (SEM) for surface and subsurface horizons of P<sub>5</sub>.

## V. Conclusions:

Cementing agents (carbonate minerals, free iron oxides and organic matter) affect on soil structure, and this reflects on shape and size distribution of soil pores related on saturated hydraulic conductivity. The micro morphological characteristic helps to describe pore configuration and explain flow processes, and reveal the common shapes of voids.

## References

- [1] D. Hillel. "Introduction to Soil Physics" Academic press, Inc. San Diego, California. (1982).
- [2] D. Johnson, F. Arriaga and B. Lowery "Automation of galling head permeameter for rapid determination of hydraulic conductivity multiple samples" *Soil Sci. Soc. Am. J.* 69: 828 – 833, (2005).
- [3] D. Hillel. "Introduction to Environmental Soil Physics" Academic press, Inc. Burlington, Massachusetts, USA, (2004).
- [4] M. Lado, A. Paz, and M. Ben-Hur "Organic matter and aggregate-size interactions in saturated hydraulic conductivity" *Soil Sci. Soc. Am. J.* 68:234 – 242, (2004).
- [5] W. Rawls, A. Nemes and A. Pachepsky "Effect of soil organic matter on soil hydraulic properties" pp. 95 – 114, (2005).
- [6] R. Hatano, N. Kawamura, J. Ikeda, and T. Sakuma "Evaluation of the effect of morphological features of flow paths on solute transport by using fractal dimensions of methylene blue staining pattern" *Geoderma.* (53), pp. 31–44 (1992).
- [7] J. Vanderborght, P. Gähwiler, H. Wydler, U. Schultze, and H. Flußler "Imaging fluorescent dye concentrations on soil surfaces: uncertainty of concentration estimates" *Soil Sci. Soc. Am. J.* (66), pp. 760–776, (2002).
- [8] A. Tarquis, K. McInnes, J. Key, A. Saa, M. García, and, M. Díaz "Multiscaling analysis in a structured clay soil using 2D images" *J. Hydrol.* (322), pp. 236–246, (2006).
- [9] R. Protz, M. Shipitalo, A. Mermut, and C. Fox "Image analysis of soils present and future" *Geoderma.* (40), pp. 115–125, (1987).
- [10] G. Cervantes, I. Sanchez-Cohen., and J. P. Rossignol "Soil water dynamics studies using image analysis" In: *Proceedings of the First Interagency Conference on Research in the Watersheds (ICRW)*, Benson, Arizona, USA, 27–30 October, pp. 263–271, (2003).
- [11] D. Holtham, P. Matthews, and D. Scholefield "Measurement and simulation of void structure and hydraulic changes caused by root-induced soil structuring under white clover compared to ryegrass" *Geoderma.* (142), pp. 142–151, (2007).
- [12] S. Ismail, "Micromorphometric Soil Porosity Characterization by Means of Electro-Optical Image Analysis (Quantimet 720)" *Soil Survey Institute, Wageningen*, (1975)

- [13] C. Murphy, P. Bullock, and R. Turner "The measurement and characterization of voids in soil thin sections by image analysis" I. Principles and techniques. *J. Soil Sci.* (28), pp. 498–508, (1977).
- [14] I. Forrer, A. Papritz, R. Kasteel, H. Fluhler, and F. Luca "Quantifying dye tracers in soil profiles by image processing" *Eur. J. Soil Sci.* (51), pp. 313–322, (2000).
- [15] C. Duwig, P. Delmas, K. Muller, B. Prado, H. Morin, and K. Ren "Quantifying fluorescent tracer distribution in allophanic soils to image solute transport" *Eur. J. Soil Sci.* (59), pp. 94–102, (2008).
- [16] R. Brewer, "Fabric and Mineral Analysis of Soil" John Wiley and Sons, New York, USA, (1964).
- [17] J. Bouma, A. Jongerius, and D. Schoonderbeek "Calculation of saturated hydraulic conductivity of some pedal clay soils using micromorphometric data" *Soil Sci. Soc. Am. J.* (43), pp. 261–264, (1979).
- [18] B. Prado, C. Duwig, J. Marquez, P. Delmas, P. Morales, J. James, and J. Etchevers "Image processing-based study of soil porosity and its effect on water movement through andosol intact columns" *Agricultural Water Management*, (96), pp. 1377–1386, (2009).
- [19] Soil Survey Staff, "Soil Taxonomy: A basic system of soil classification" *Soil Survey Agric. Handbook NO.436*, U.S. Government Printing Office Washington D.G., (1975).
- [20] A. Klute, "Water retention: Laboratory methods" In: Klute, A., ed., "Methods of Soil Analysis, Part 1: Physical and Mineralogical Methods," Monograph No. 9. Am. Soc. Agron., Madison, WI. (1986).
- [21] M. Jackson, "Chemical Composition of Soils" Inf. E. Bear (ed). *Chemistry of the soil*. Van No strant Reinhold Co. New York, (1964).
- [22] M. Jackson, "Soil Chemical Analysis" Pretrice-hall Inc. Englewood, Cliffs, N. J. (1958).
- [23] P. Hesse, "A Text book of Soil Chemical Analysis" John Murray Ltd. Great Britain, (1972).
- [24] O. Mehra, and M. Jackson "Iron Oxide Removal from Soils AND Clay by Dithionite-Citrate System Buffered with Sodium Bicarbonate" *Proceeding of 7th National Conference on Clays and Clay Minerals*, pp. 317 – 327, (1960).
- [25] SAS Institute Inc., "SAS Users Guide" SAS Institute Inc., Cary, NC, USA (2000).
- [26] Y. Kadir, I. Celik, S. Kapur, and J. Ryan "Clay Minerals, Ca/Mg Ratio and Fe-Al-Oxides in Relation to Structural Stability, Hydraulic Conductivity and Soil Erosion in Southeastern Turkey" *Turk. J. Agric. For.* (29), pp. 29 – 37, (2005).
- [27] I. Shainberg, and M. J. Singer "Soil response to saline and sodic condition" In: *Agricultural salinity Assessment and Management*. (Ed:K. K. Tanjity) Am. Soc. Cical Eng., st Josephs, USA, pp. 91 – 112, (1990).

[28] K. Dontsova, and L. Norton "Clay dispersion, infiltration, and erosion as influenced by exchangeable Ca and Mg. *Soil Sci. Soc. Am. J.* (167), pp. 184 – 193, (2002).

[29] R. Kodesova, V. Kodes, and A. Sim-Nek "Soil micromorphology, soil structure stability and soil hydraulic properties" *Plant, Soil and Environment*, (51), PP. 310-315, (2006).

[30] S. Duiker, F. Rhoton, J. Torrent, N. E. Smeck and R. Lal " Iron (hydroxide) crystallinity effects on soil aggregation" *Soil Sci. Soc. Am. J.*, (67), PP. 606 – 611, (2003).